J6.3 REFINEMENT OF NUMERICAL MODELING AND TECHNOLOGY OF GLOBAL AND REGIONAL WATER CYCLE

Hiromasa Ueda*

Disaster Prevention Research Institute, Kyoto University, Uji, Japan

Toshio Yamagata

Department of Earth and Planetary Science, Graduate School of Science
The University of Tokyo, Tokyo, Japan,
and Frontier Research Center for Global Change/JAMSTEC, YES, Yokohama, Japan

Ryohji Ohba

Mitsubishi Nagasaki R&D Centre, Mitsubishi Heavy Industry Ltd., Nagasaki, Japan

Hirofumi Sakuma

Frontier Research Center for Global Change/JAMSTEC, YES, Yokohama, Japan

Swadhin K. Behera

Frontier Research Center for Global Change/JAMSTEC, YES, Yokohama, Japan

Milind Mujumdar

Indian Institute of Tropical Meteorology, Pune, India,

Arun Chakraborty

Department of Earth and Planetary Science, Graduate School of Science,
The University of Tokyo, Tokyo, Japan and
Advanced Technology Research Center, Mitsubishi Heavy Industry Ltd., Kanagawa, Japan

1. INTRODUCTION

Japan Ministry of Education, Culture, Sport, Science and Technology (MEXT) started a new national research mission for the sustainable coexistence of human, nature and the earth. Under the auspices of this revolutionary research plan, we undertake a project entitled “Advanced Prediction System and Counter Measures of Regional- and Meso-scale Water Cycle” (Global Water Cycle Project). The purpose of this project is to make a master plan for the improvement of desert environment. This project will continue from March 2002 until March 2007. In the interdisciplinary project initiated by MEXT Mitsubishi Heavy Industries (MHI) plays a central role in organizing the multifaceted project involving industry and research organizations; Frontier Research Centre for Global Change (FRCGC), National Research Institute of Earth Science and Disaster Prevention (NRIESDP), Kyoto University, Tottori University and Sophia University in Japan.

*Corresponding author address: Prof. Hiromasa Ueda, *Disaster Prevention Research Institute, Kyoto University Uji City, Kyoto – 611 0011*, Japan. E-mail: ueda@storm.dpri.kyoto-u.ac.jp

The FRCGC studies the mechanism of rainfall in coastal desert to understand and predict desert climate variability using a global model on the Earth Simulator. The NRIESDP and Kyoto University develop the integrated regional hydrological cycle model and predicts hydrological cycle and its variability. MHI develops the new technology for water resources by sustainable energy, such as solar power. Tottori University develops water recycling-based reforestation, accretion of residential space, development of biological production system. Sophia University evaluates environmental impacts introduced by environmental improvement of coastal desert and its impact on human life. Here we introduce some of our preliminary results based on the analyses of atmospheric reanalysis data and the model results.

The understanding of global and regional hydrological cycle is an important area of climate variability research. A simple hydrological cycle involves evaporation from the continental water bodies and oceans and transportation of water vapor to the neighboring regions. The water vapor flux helps in precipitation onto the land surface, which then flows back into the oceans as river flow. During this cycle, some parts of precipitated water over the land evaporate again and contribute to another cycle of precipitation.

The variability of the atmospheric water vapor flux is caused by the variations of the regional and global circulation patterns due to the tropical and extra-tropical climatic events (El Niño/Southern Oscillation, Indian Ocean Dipole, North Atlantic Oscillation etc.). It is very important to understand the variability of water vapor flux for the water cycle of semi-arid region like Saudi Arabia (Fig. 1a), where the scarcity of water critically affects the regional climate. It is also important to understand the atmospheric moisture budget of this region for arid region management and desert amelioration projects.

The El Niño/ Southern Oscillation (ENSO) and recently discovered Indian Ocean Dipole (IOD) are two important manifestation of the tropical air-sea interaction (Saji et al. 1999; Webster et al. 1999; Yamagata et al. 2004). The impact of ENSO on the monsoon climate is well established (Walker 1923; Shukla and Paolino 1983; Joseph et al. 1994). The existence of subtropical deserts (viz. Sahara) has often been attributed to the annual and zonal mean Hadley circulation which shows strong decent in the subtropics. However, the zonal-mean Hadley circulation shows considerable evolution over the course of the year with very strong subtropical decent during winter, but practically no zonal-mean subtropical decent during summer when rainfall over eastern Sahara and the Mediterranean is the lowest. Rodwell and Hoskins (1996) introduced the monsoon-desert mechanism for desertification using numerical experiment which shows remote diabatic heating in the Asian monsoon region can induce a Rossby-wave pattern to the west. With their mechanism, desertification can be forced by remote changes in monsoon strength rather than by local effects. It explains the aridity of east Sahara/Mediterranean - Kyzylkum desert regions. They also mention that the Arabian Desert is less well explained by their mechanism. However, they observed weak vertical motion over this region in their analysis. The IOD events also have a strong influence on the climate not only the immediate neighboring East African and Indonesian regions (Saji et al. 1999; Behera et al. 2004a) but also the Indian summer monsoon region (Behera et al. 1999; Ashok et al. 2001), East Asia (Saji and Yamagata 2003; Yamagata et al. 2003a; Guan et al. 2003), the Mediterranean, Australia and Brazil (Saji and Yamagata 2003).

The above studies reveal that there is a possible influence of IOD and ENSO on the Saudi Arabian climate but no such literature is available with detail description in recent times. Therefore, the objective of this paper is to understand the role of IOD and ENSO on the moisture budget over Saudi Arabia. We have diagnosed the 43-year record of moisture flux from NCEP/NCAR reanalysis datasets and also rainfall from the Global Precipitation Climatology Project (GPCP). Besides the diagnosis of the atmospheric data, we conducted some regional model simulation with a very high resolution (1km X 1km) in Arabian Peninsula in order to understand the possibility of rain enhancement by greening the desert area with a low grass.

The paper is organized as follows. The brief description of the model datasets and methodology are presented in section 2. In section 3, the results and discussions of the analysis of NCEP/NCAR reanalysis along with our model results are presented. Conclusions are given in section 4.

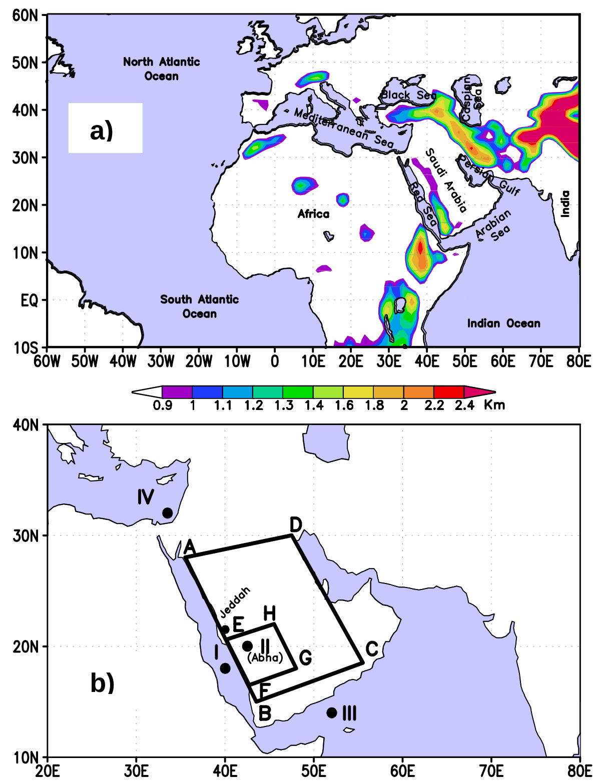

Fig. 1. (a) Diagram showing the adjacent seas of Saudi Arabia along with topography, (b) The domain of selected regions studied in this paper (Area I: over Red Sea; Area II: over Abha; Area III: over Arabian Sea and Area IV: over Mediterranean Sea).

2. DATA, MODEL AND METHODOLOGY

The NCEP/NCAR reanalysis datasets (Kalnay et al. 1996) of 43-year period from 1958 to 2000 are used in this study. We use GISST dataset (Rayner et al. 1996) for the same period to compute the dipole mode index (DMI) as in Saji et al. (1999) and Niño-3 index (obtained by taking the area-average of SST anomalies over 5°N – 5°S, 150°W – 90°W). Rainfall data from Xie and Arkin (1997), Willmott et al. (1996) and station observations (obtained from Meteorological and Environmental Protection Agency (MEPA) of Saudi Arabia) are also used in our study. Domains and regions considered in our study are shown in Fig. (1b). For the analysis of Arabian Cyclone, the GPCP(*http://precip.gsfc.nasa.gov/gpcp_daily_comb.html)* daily rainfall data is used for detailed analysis of the evolution of the large-scale rainfall events for the period from 1997 through 2002. This global 1°x1° daily rainfall estimate are based on gauge and satellite observations.

3. RESULTS AND DISCUSSIONS

3.1 Seasonal variability in local and regional moisture flux

The distribution of net incoming moisture flux (Fig. 2a) shows a semi-annual signal with a larger peak in winter (November – April) and another much smaller maximum in summer (June – August) (Chakraborty et al. 2004). This is observed both in ABCD (whole Saudi Arabia) and EFGH (only Abha and surrounding region) domains (Fig. 1b). It is also seen that summer peaks for both domains are identical. This indicates that most of the incoming moisture flux concentrates on the Abha region. Thus, the summer time rain peak (Fig. 2b) is expected near Abha (Behera et al. 2004b). The local convection is explained by orographic lifting of warm and moist air associated with monsoon winds, which pass through the Red Sea as discussed in the previous section. In contrast, the winter peak of the ABCD domain is much larger than that of the EFGH, indicating a wide spread rainfall over Saudi Arabia. The winter time moisture flux is associated with the enhancement of eastward propagating Mediterranean disturbances near the Abha region by the local effects of orography and moist air advection from the Red Sea (Mujumdar et al. 2004). For other months of the year, however, the net moisture flux over these domains are near zero or negative. In agreement with the net moisture flux, the rainfall estimates over the mountainous region of the Asir Province (Abha) also show similar semi-annual signal (Fig 2b).

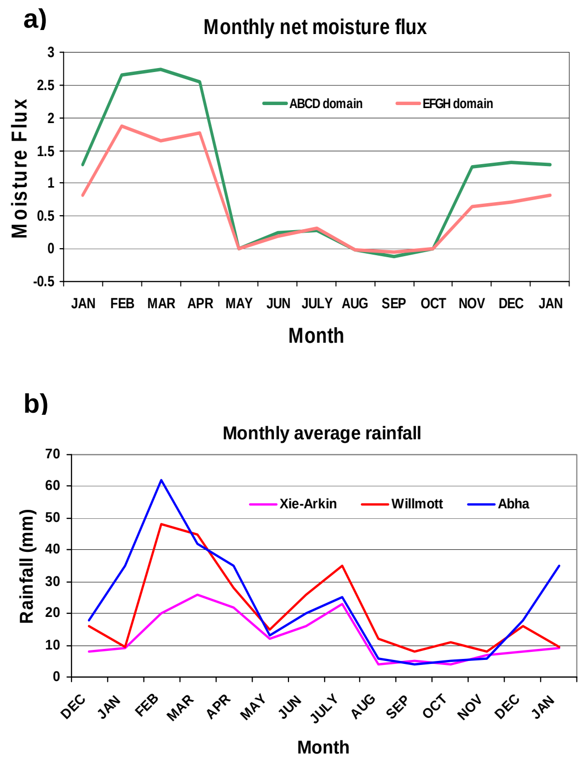

Fig. 2. (a) Seasonal variation of net moisture flux, and (b) average monthly rainfall over south-western Saudi Arabia (Xie – Arkin and Willmott) and Abha region.

3.2 Interannual variability of moisture flux

We examine the interannual variability of the moisture flux. In particular, we focus on possible relations with the tropical climate phenomena like the IOD and the ENSO. The interannual variability of the incoming moisture flux across the walls of ABCD and EFGH domains are shown in Fig. 3. We have adopted a 5-month running mean here. Significant variability in the moisture flux is seen during 1960 – 67 and 1980 - 2000. It is weak during 1968 - 79. During the IOD (1961, 1994, and 1997) and ENSO (1963-64, 1982-83, 1987-88, and 1997-98) events, the impact is even larger than the normal years except for 1968 - 79. The weak variability during 1968 - 79 may be associated with the period of weak variation of IOD (Behera and Yamagata 2003). During positive IOD events the incoming moisture flux across the Red Sea side (AB or EF) increases (Fig. 3). This influx helps the net gain of moisture but is slightly offset by the weak outflux across the

Persian Gulf side (CD/GH). The partial lag correlation with moisture flux from the Red Sea side shows that a positive IOD (El Niño) event has a peak correlation coefficient of about 0.5 (0.6) with 5 (2) months lead.

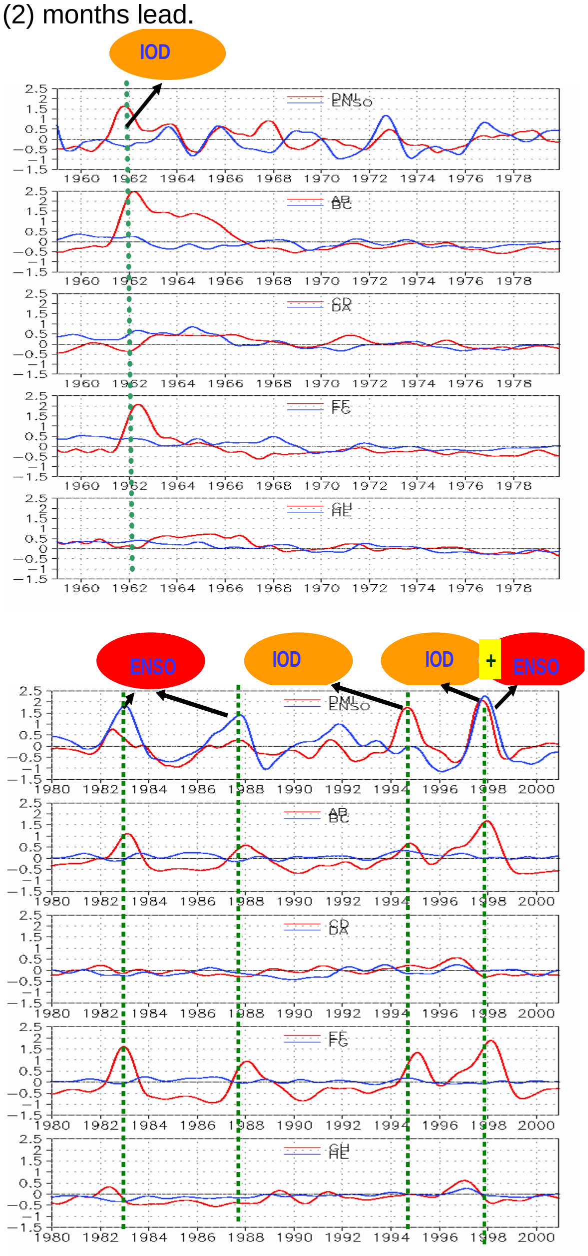

Fig. 3. Interannual variations of moisture flux indices across the walls shown in Fig. 1b and its comparison with IOD and ENSO.

During an El Niño event the characteristic of the moisture flux across the Red Sea and Arabian Sea sides is somewhat different as compared to positive IOD event (Fig. 4). During pure IOD event (e.g. 1961 and 1994) (Yamagata et al. 2002,2003b), the transport is from Sudan region and reaches the study region through the Red Sea side. This type of transport is locally known as the Sudanese wave (Abdullah and Al-Mazroui 1998.). The eastward tropical flow during the pure positive IOD event causes moisture convergence over the southwestern Arabian region (Fig. 4a). The local orographic ascent in Asir Province leads to an increase in rainfall activity. The large-scale subsidence over the western Indian Ocean during the pure El Niño event (e.g. 1987) also causes the local convergence of moisture over the southwestern Arabian region (Fig. 4b). When positive IOD and warm ENSO occur concurrently (Fig. 4c), the convergence of moisture flux is enhanced owing to the combined contribution of large-scale circulation from positive IOD and warm ENSO. Because of anomalous cyclonic circulation over the northwestern Saudi Arabia which blocks the outflow towards Persian Gulf, the local moisture convergence over southwestern Arabian region is enhanced and, as a result, rainfall activity is increased.

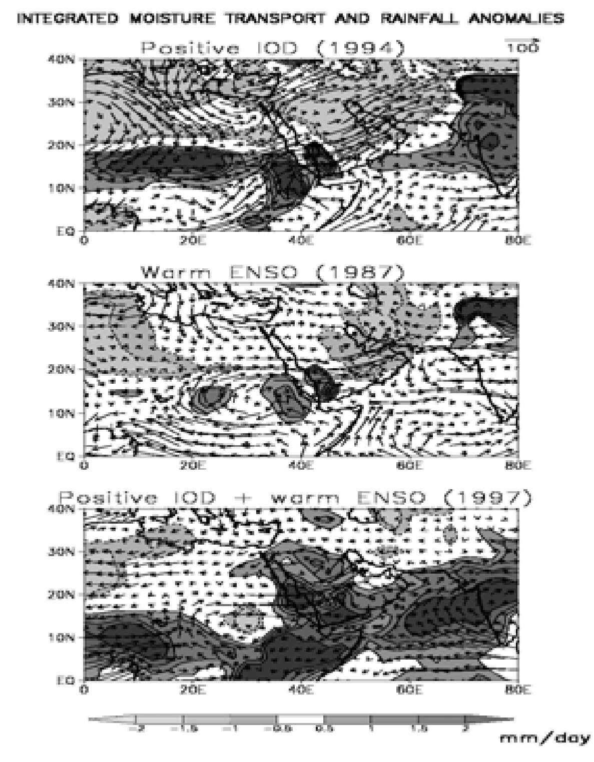

Fig. 4. Anomalies of vertically integrated moisture flux anomalies (NCEP/NCAR). The shaded values are rainfall anomalies (Xie –Arkin) for three special years for November-January.

3.3 Origin of the synoptic weather disturbances

The daily rainfall distribution is analyzed over the Saudi Arabian region and its neighborhood in winter to identify Arabian rainfall events. Visual examination of the GPCP data showed two active rainfall regions around Mecca of the Province of Asir and around Basra located near the northern edge of the Persian Gulf. Both Mecca and Basra regions have a number of rain gauge stations, which provide better ground truth for the satellite data. When the rainfall over Mecca (around 20°N, 42°E) and Basra (around 30°N, 47°E) regions exceeds a threshold value of 5 mm/day within a grid box of 5^0x5^0, i.e. one standard deviation of the wintertime rainfall, the rain event is considered as a significant rainfall event. A slight change in the location of the grid box does not influence the definition of the Arabian rainfall events. We thus identify 19 Arabian rainfall events during January, February and March for the period from 1997 through 2002. The number of events is enough for statistical significance of the present analysis.

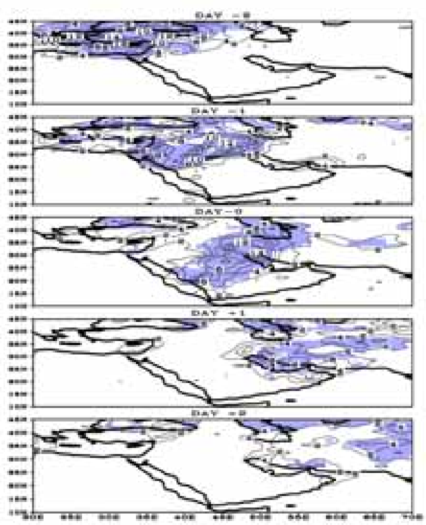

Fig. 5. Composite maps of time evolution of Arabian rainfall events (unit mm/day; contour interval is 2units) during January. The shaded region overlying contours of precipitation corresponds to the statistical significance exceeding 90% of confidence level (from 2-tailed Student's t-test).

In order to examine the spatial distribution of Arabian rainfall events we have prepared composite maps based on the identified Arabian rainfall events during January, February and March. The evolution of the event is examined by extending the composite analysis to days prior and after the occurrence of the significant events on Day 0. The composites preceding the Day 0 are noted as Day -1, Day -2 and composites following the Day 0 are noted as Day +1, Day +2. Figure 5 shows the heavy precipitation area around the Mediterranean region from Day -2 to Day 0. The precipitation area moves southeastward from Day -2 and covers the northern part of the Red Sea and adjacent continental Arabia on Day -1. On Day 0, the rainfall area extends from the Red Sea adjacent to Mecca to the southern part of the Caspian Sea. Two rainfall maxima are found over the region of our analysis: a major maximum one over Basra and a minor maximum over Mecca. The major maximum, which lies to the west of the mountainous region of Iran, is stronger and well spread as compared to the minor one that lies near Mecca. We note here that the strong precipitation over Basra starts one day prior (on Day -1) to significant rainfall over Mecca. Following the Day 0 event, convective activity becomes weaker and moves northeastward toward the high altitude region of Iran on Day +1 and continues to move eastward on Day +2, covering parts of northwest India.

The composites in February and March (figure not shown) show a striking similarity in the spatial distribution of rainfall as compared to those in January shown in Fig.5. We note, however, that the east-west extent is narrower in February and March as compared to that in January. The amplitudes of two rainfall maxima are also weaker during February and March.

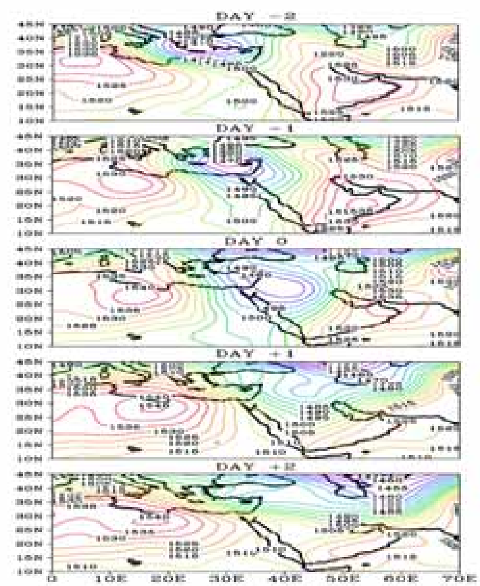

Fig. 6. Time sequence of geopotential height at 850 hPa (Contour interval is 10 hPa).

The evolution of the weather disturbances bringing the synoptic Arabian rainfall events is diagnosed from the time sequence of atmospheric variables, e.g., mean sea level pressure, geopotential height, vertical velocity, and moisture transport. The surface and lower tropospheric features suggest that the convection system associated with the rainfall events starts from the Mediterranean Sea and its adjacent Middle East region 2 days prior (Day -2) to the significant events in Saudi Arabia. The precipitation events are associated with eastward propagating mid-latitude weather disturbances: geopotential height in Fig. 6 shows that the transient system moves in a waveform with a low pressure preceded by a high. The low pressure extends over the Red Sea and the wide region of Saudi Arabia with the southeastward shift of the center of low pressure and thereby shifting the preceding high pressure to further east on Day 0. The northwesterly associated with the cyclone is called "*winter shamal*". A strong gradient in the geopotential heights develop on the eastern front of the low pressure due to the blocking effect of high pressure to the east (Fig.6). This gradient causes an anomalous low level jet from Red Sea to the Persian Gulf on Day 0. Figure 7 depicts the associated moisture influx from the Red Sea to the interior of Saudi Arabia.

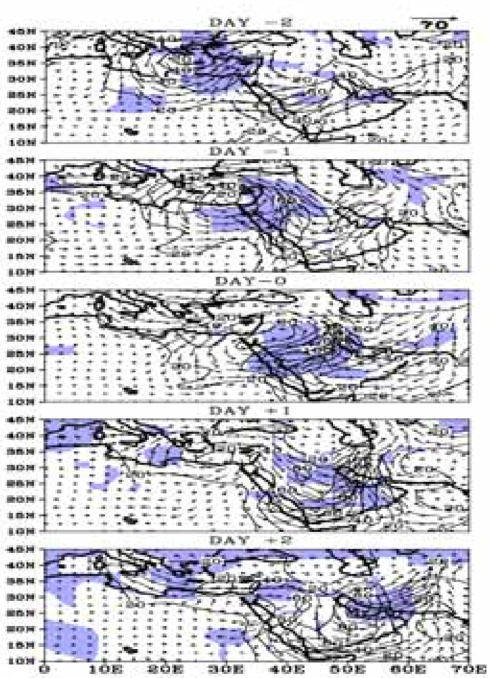

Fig. 7. Composite maps of time evolution of moisture transport anomalies during January.

The anomalous moisture transport vector captures the distribution of anomalous moisture convergence over the Mediterranean Sea and the adjoining area on Day-2. The enhanced moisture transport pattern is consistent with the significant rainfall pattern over the region. A remarkable feature on Day-1 is the band of anomalous moisture influx elongated southeastward over the Red Sea and the adjacent continental Arabia. The enhancement of moisture transport over the mountainous region of the Province of Asir on Day 0 is due to strengthened convergence over the Red Sea around 20°N, which leads to the significant rainfall event on Day 0. On Day +1 the moisture flux is further enhanced over the high-altitude region of Iran and, on Day +2, the area of enhanced convection spreads further eastward up to the north-west region of India.

This well-defined weather system has characteristic of a synoptic scale mid-latitude cyclone (e.g. Holton 1992; Trigo et. al. 2002). The horizontal scale of the system is of the order of 1000 km and a well marked trough is found at 200 hPa (supplementary figure) to the west of the low pressure system. A core of maximum positive relative vorticity is found in the meridional-height cross-section along 40°E, which suggests the influence of the upper level trough on the surface conditions. Several previous studies already discussed the importance of upper level trough in the development of low level cyclogenesis over the Mediterranean region (e.g. Jacobeit 1987; Flocas and Karacostas 1996). Most of these midlatitude disturbances travel eastward north of the Middle East region due to the dominance of wintertime high over the Arabian Peninsula. However there are occasions, particularly in January, when the mid-latitude transient disturbances reach their southernmost latitude around the Mediterranean Sea region (Trigo et. al. 2002) and last for four to five days (Julian 1971; Hartmann 1974).

4. CONCLUSIONS

The results obtained from studies during 2002 and 2003 are very encouraging for the desert amelioration project. The tropical climate variability from the Indian and Pacific Oceans, viz. the Indian Ocean Dipole (IOD) and the El Nino/ Southern Oscillation (ENSO), are found to dominantly influence the rainfall patterns through the atmospheric teleconnections. The seasonal variation of net moisture shows a prominent semi-annual signal with the highest peak during February – April and another smaller peak during

June – August. The seasonal gain of moisture in summer does not vary between the smaller region of Asir Province (EFGH) and the whole Saudi Arabia (ABCD) explaining the higher rainfall during summer confined only to Asir Province. The moisture gain over a wider area (ABCD) compared to the smaller domain (EFGH) explains widespread rain during winter and spring.

The interannual variation of moisture flux shows that it is strongly modified by the tropical climate phenomenon like the positive IOD and the warm ENSO events. During these climate events, the transport of moisture from the Red Sea toward the mountainous region of Asir Province enhances and, as a result, the rainfall during November to April increases. The impact on the moisture transport to the Saudi Arabian region from the Red Sea side (AB and EF) for both the positive IOD and the warm ENSO events is stronger than other sides. The positive IOD and warm ENSO show highest correlations with moisture flux from the Red Sea side. It is shown that vertically integrated moisture flux anomalies increases towards Saudi Arabia across the Red Sea during a pure positive IOD, warm ENSO and concurrent positive IOD and warm ENSO years. It is also noted that concurrent positive IOD and warm ENSO year contribution of moisture flux to the Saudi Arabian region through the Red Sea side is larger than that of pure positive IOD year or pure warm ENSO year. It is also evident that during pure positive IOD year both the South Atlantic Ocean and the North Atlantic Ocean contribute moisture over Saudi Arabia, while, during ENSO year, the South Atlantic mainly contributes.

The large impact of positive IOD and warm ENSO on the interannual variability of the incoming moisture flux over Saudi Arabia, and possible rain enhancement over Saudi Arabia by greening the desert area with low grasses are two main findings of our study. This is important for the understanding of climate impact in desert amelioration.

Using GPCP and NCEP/NCAR data sets the evolution of wintertime Arabian Cyclones that are traced back to the Mediterranean region is another finding of our study. In order to deepen our understanding on the structure and dynamics of those Arabian Cyclones analyses and sensitivity experiments with very high resolution regional model simulation is currently underway. Also the most high-speed computer in the world, called the "Earth Simulator" provides us a scope to resolve complicated terrains and complex surface conditions in supper-high resolution (1km x 1km) in Arabian Peninsula. The results of preliminary simulations indicate that there is a possibility of rain enhancement by greening the desert area of 5625 square kilometers with low grass.

Acknowledgements: This study is supported by Ministry of Education, Culture, Sports, Science and Technology of JAPAN through Mitsubishi Heavy Industries Ltd. We are thankful to Mr. M. Harada, Mr. K. Muta, Dr. K. Baba, Mrs. Hoeller and Mrs. Moriyama for their support in carrying out this research. The discussions and suggestions provided by Drs. Tomoki Tozuka, R. Suzuki, H. Nakamura, Y. Masumoto and scientists from FRCGC are greatly acknowledged.

References:

Abdullah, M. A, and M.A. Al-Mazroui, 1998: Climatological study of the southwestern region of Saudi Arabia. I. Rainfall analysis. Clim. Res. 9, 213-333.

Ashok, K., Z. Guan, and T. Yamagata, 2001: Impact of the Indian Ocean Dipole on the relationship between the Indian Monsoon rainfall and ENSO. *Geophys. Res. Lett.*, **26**, 4499 – 4502.

Behera, S. K., R. Krishnan, and T. Yamagata, 1999: Unusual Ocean-Atmosphere conditions in the tropical Indian Ocean during 1994. *Geophys. Res. Lett.*, **26**, 3001-3004.

Behera, S. K., and T. Yamagata, 2003: Influence of the Indian Ocean Dipole on the Southern Oscillation. *J. Meteorol. Soc. Japan*, **81 (1)**, 169 – 177.

Behera, S. K., J.-J. Luo, S. Masson, P. Delecluse, S. Gualdi, and A. Navarra, T. Yamagata, 2004a: Paramount Impact of the Indian Ocean Dipole on the East African Short Rains: A CGCM Study, *J. Climate (submitted).*

Behera S.K., A. Chakraborty, M. Mujumdar, R. Ohba, and T. Yamagata, 2004b: Seasonal to interannual variability of rainfall over southwestern Saudi Arabia. *Geophys. Res. Lett.,* (under submission).

Chakraborty, A., S. K. Behera, Milind Mujumdar, R. Ohba, and T. Yamagata, 2004: Diagnosis of tropospheric moisture over Saudi Arabia and influences of IOD and ENSO. Mon. Wea. Rev. (Under revision).

Flocas, H. A., and T. S. Karacostas, 1996: Cyclogenesis over the Aegean Sea: Identifications and synoptic categories. *Meteor. Appl.,* **3,** 53–61.

Guan, Z., K. Ashok, and T. Yamagata, 2003: Summertime Response of the Tropical Atmosphere to the Indian Ocean Dipole Sea Surface Temperature Anomalies. *J. Met. Soc. Japan*, **81(3)**, 533-561.

Hartmann, D. L., 1974: Time spectral Analysis of Mid-latitude disturbance. *Mon. Wea. Rev.,* **102**, 348-362.

Holton, J.R., 1992: An Introduction to Dynamic Meteorology, 3rd ed., Academic Press.

Jacobeit, J., 1987: Variations of trough positions and precipitation patterns in the Mediterranean area. *J. Climatol.,* **7,** 453–476.

Joseph, P. V., J. K. Eischeid, and R. J. Pyle, 1994: Interannual variability of the onset of the Indian summer monsoon and its association with atmospheric features, El Nino and sea surface temperature anomalies. *J. Climate*, **7**, 81 – 105.

Julian, P.R., 1971: Some aspects of variance spectra of synoptic scale tropospheric wind components in midlatitude and in the tropics. *Mon. Wea. Rev.,* **99**, 954-965.

Kalnay, E. and coauthors, 1996: The NCEP/NCAR Reanalysis Project. *Bull. Amer. Meteor. Soc.,* **77**, 437-471.

Mujumdar, M., S. Behera, A. Chakraborty, T. Miyasaka, T. Tozuka, R. Ohba, and T. Yamagata, 2004: Wintertime Arabian rainfall events, *Geophys. Res. Lett.* (Communicated).

Rayner, N. A., E. B. Horton, d. E. Parker, C. K. Folland, and R. B. Hackett, 1996: Version 2.2 of the Global sea-Ice and Sea Surface Temperature Data Set, 1903 – 1994, Climate Research Technical Note 74, Hadley Centre for Climate Prediction and Research, London Road, Bracknell, RG12 2SY, UK.

Rodwell, M. R. and B. J. Hoskins, 1996: Monsoons and the dynamics of deserts. *Q. J. R. Meteorol. Soc*., **122**, 1385 - 1404.

Saji, N. H., B. N. Goswami, P. N. Vinayachandran, and T. Yamagata, 1999: A dipole mode in the tropical Indian Ocean. *Nature***, 401**, 360 – 363.

Saji, N.H., and T. Yamagata, 2003: Possible impacts of Indian Ocean Dipole mode events on global climate. *Clim. Res*., **25 (2)**, 151-169.

Shukla, J., and D. Paolino, 1983: The southern oscillation and long-range forecasting of summer monsoon rainfall over India. *Mon. Wea. Rev*., **111**, 1830 – 1837.

Trigo I. F., Bigg G. R. and Davis T. D., 2002: Climatology of cyclogenesis mechanisms in the Mediterranean. *Mon. Wea. Rev*., **130**, 549-569.

Walker, G. T., 1923: Correlation in seasonal variations of weather, VIII: A preliminary study of world weather. *Mem. Indian Meteorol. Dept*., **24**, 75 – 131.

Webster, P. J., A. Moore, J. Loschnigg, and M. Leban, 1999: Coupled ocean-atmosphere dynamics in the Indian Ocean during 1997-98. *Nature*, **40**, 356-360.

Willmott, C.J., S.M. Robeson and M.J. Janis, 1996: Comparison of Approaches for Estimating Time-Averaged Precipitation Using Data from the USA. *International Journal of Climatology*, 16, 1103-1115.

Xie, P. and P. A. Arkin, 1997: Global precipitation: A 17-year monthly analysis based on gauge observations, satellite estimates and numerical model outputs. *Bull. Amer. Met. Soc.*, 78, 2539-2558.

Yamagata, T., S. K. Behera, S. A. Rao., Z. Guan, K. Ashok, and H. N. Saji, 2002: The Indian Ocean dipole: a physical entity, *CLIVAR Exchanges, 24***,** 15-18.

Yamagata, T., S. K. Behera, S. A. Rao, Z. Guan, K. Ashok, and H. N. Saji, 2003a: Comments on “Dipoles, Temperature Gradient, and Tropical Climate Anomalies”, *Bull. Am. Meteorol. Soc., 84*, 1418-1422.

Yamagata, T., S.K.Behera, Z.Guan, 2003b: The role of the Indian Ocean in climate forecasting with a particular emphasis on summer conditions in East Asia. Proceedings of the ECMWF Workshop on the Role of the Upper Ocean in Medium and Extended Range Forecasting, 102-114.

Yamagata, T., S. K. Behera, J. -J. Luo, S. Masson, M. Jury, and S. A. Rao, 2004: Coupled ocean atmosphere variability in the tropical Indian Ocean, *AGU Monograph “Ocean-Atmosphere Interaction and Climate Variability”* Ed Wang, Xie and Carton, Vol. 147, pp 414.